

1-21-2013

Gambogic Acid Is a Tissue-Specific Proteasome Inhibitor In Vitro and In Vivo

Xiaofen Li

Guangzhou Medical College, China

Shouting Liu

Guangzhou Medical College, China

Hongbiao Huang

Guangzhou Medical College, China

Ningning Liu

Guangzhou Medical College, China

Chong Zhao

Guangzhou Medical College, China

See next page for additional authors

Recommended Citation

Li, X., Liu, S., Huang, H., et al. 2013. Gambogic Acid Is a Tissue-Specific Proteasome Inhibitor In Vitro and In Vivo. *Cell Reports*, 3(1): 211-222. DOI: 10.1016/j.celrep.2012.11.023

Available at: http://digitalcommons.wayne.edu/med_oncology/1

Authors

Xiaofen Li, Shouting Liu, Hongbiao Huang, Ningning Liu, Chong Zhao, Siyan Liao, Changshan Yang, Yurong Liu, Canguo Zhao, Shujue Li, Xiaoyu Lu, Chunjiao Liu, Lixia Guan, Kai Zhao, Xiaoqing Shi, Wenbin Song, Ping Zhou, Xiaoxian Dong, Haiping Guo, Guanmei Wen, Change Zhang, Lili Jiang, Ningfang Ma, Bing Li, Shunqing Wang, Huo Tan, Xuejun Wang, Q. Ping Dou, and Jinbao Lin

Gambogic Acid Is a Tissue-Specific Proteasome Inhibitor In Vitro and In Vivo

Xiaofen Li,^{1,6} Shouting Liu,^{1,6} Hongbiao Huang,^{1,6} Ningning Liu,^{1,6} Chong Zhao,^{1,6} Siyan Liao,^{1,6} Changshan Yang,¹ Yurong Liu,¹ Canguo Zhao,¹ Shujue Li,^{1,3} Xiaoyu Lu,¹ Chunjiao Liu,¹ Lixia Guan,¹ Kai Zhao,¹ Xiaoqing Shi,¹ Wenbin Song,¹ Ping Zhou,¹ Xiaoxian Dong,¹ Haiping Guo,¹ Guanmei Wen,¹ Change Zhang,¹ Lili Jiang,¹ Ningfang Ma,¹ Bing Li,² Shunqing Wang,¹ Huo Tan,¹ Xuejun Wang,⁴ Q. Ping Dou,^{5,*} and Jinbao Liu^{1,*}

¹Protein Modification and Degradation Lab, Department of Pathophysiology

²Experiment Medical Research Center

Guangzhou Medical College, Guangzhou, Guangdong 510182, China

³Guangdong Provincial Key Lab of Urology, Department of Urology, Minimally Invasive Surgery Center, The First Affiliated Hospital, Guangzhou Medical College, Guangzhou, Guangdong 510230, China

⁴Division of Basic Biomedical Sciences, Sanford School of Medicine of the University of South Dakota, Vermillion, SD 57069, USA

⁵The Molecular Therapeutics Program, Barbara Ann Karmanos Cancer Institute, and Departments of Oncology, Pharmacology and Pathology, School of Medicine, Wayne State University, Detroit, MI 48201-2013, USA

⁶These authors contributed equally to this work

*Correspondence: doup@karmanos.org (Q.P.D.), liujinbao1@yahoo.com.cn (J.L.)

<http://dx.doi.org/10.1016/j.celrep.2012.11.023>

SUMMARY

Gambogic acid (GA) is a natural compound derived from Chinese herbs that has been approved by the Chinese Food and Drug Administration for clinical trials in cancer patients; however, its molecular targets have not been thoroughly studied. Here, we report that GA inhibits tumor proteasome activity, with potency comparable to bortezomib but much less toxicity. First, GA acts as a prodrug and only gains proteasome-inhibitory function after being metabolized by intracellular CYP2E1. Second, GA-induced proteasome inhibition is a prerequisite for its cytotoxicity and anticancer effect without off-targets. Finally, because expression of the CYP2E1 gene is very high in tumor tissues but low in many normal tissues, GA could therefore produce tissue-specific proteasome inhibition and tumor-specific toxicity, with clinical significance for designing novel strategies for cancer treatment.

INTRODUCTION

Gambogic acid (GA) is the principal pigment of gamboge resin of several *Garcinia* species. The gamboge resin has been used as a coloring material and traditional Chinese medicine for the treatment of human diseases (Gruenwald and Jaenicke, 2000). Recent studies have demonstrated that GA has anticancer effects and inhibits the growth of multiple types of human cancer cells in vitro and in vivo (Zhang et al., 2004; Pandey et al., 2007; Yi et al., 2008). GA has been approved by the Chinese Food and Drug Administration for the treatment of different cancers in clinical trials (Zhou and Wan, 2007).

In both animal tumor models and clinical trials, GA efficiently inhibits tumor growth with minimal side effects, with little toxicity on immune and hemopoietic systems (Guo et al., 2003; Zhou and Wan, 2007). Thus, identification of the specific molecular targets responsible for GA-mediated anticancer effect should have great clinical significance. Some potential molecular targets of GA have been reported that may contribute to its cytotoxicity and anticancer activity, including binding to the transferrin receptor and suppressing nuclear factor- κ B (NF- κ B) signaling pathway (Pandey et al., 2007) and inhibiting VEGFR2 (Yi et al., 2008).

Intracellular P450 is mainly responsible for the metabolism of GA (Liu et al., 2006). The metabolites of GA have been well studied in vivo and in vitro. In rat liver microsomes, GA is rapidly metabolized to two phase I metabolites, MT₁ and MT₂ (Liu et al., 2006). MT₁ and MT₂ are probably the epoxide metabolite and hydration metabolite of GA, respectively. Other phase II metabolites of GA were also identified in rat bile, such as 9,10-epoxy-gambogic acid-30-O-glucuronide and 10-hydroxygambogic acid-30-O-glucuronide (Feng et al., 2007). Recently two sulfonic acid metabolites of GA, 10- α sulfonic acid and 10- β sulfonic acid, were also found present abundantly in the fecal samples of rats after intravenous administration (Yang et al., 2011). However, the major circulating metabolite of GA in humans was identified to be MT₂ (Yang et al., 2010).

Bortezomib (Velcade, Vel) as the first proteasome inhibitor anticancer drug has been approved by US FDA for the treatment of multiple myeloma. However, relapses and toxicities were found to be associated with Vel treatment (Adams, 2004; Richardson et al., 2005), suggesting the need for discovery of novel proteasome inhibitors with no or low toxicity.

The current study reports the following findings: (1) proteasome is a specific molecular target of GA and GA at a therapeutic dose exerts anticancer effect through proteasome inhibition without off-targets; (2) GA is a proteasome inhibitor prodrug that is metabolized to an active proteasome inhibitor by CYP2E1; (3) due to the selective distribution of CYP2E1, GA

induces tissue-specific proteasome inhibition and cytotoxicity, an advantage over other proteasome inhibitors including Vel.

RESULTS

GA Indirectly Inhibits Proteasome Activities

Most recently, we have reported that the combination of GA with the classic proteasome inhibitor MG132 or MG262 synergistically inhibited tumor cell growth and induced cell death (Huang et al., 2011a). To elucidate the involved molecular mechanism, we measured the levels of the proteasome inhibition in human leukemia K562 cells after treatment with GA alone, MG132 or MG262 alone, or their combinations. As expected, MG132 or MG262 treatment alone inhibited proteasomal activity in K562 cells, as measured by increased levels of ubiquitinated proteins (Figure 1A, lanes 3 and 5). Surprisingly, GA alone was also able to accumulate the ubiquitinated proteins (Figure 1A, lane 2), which was dose dependent (Figure 1B). Most importantly, the combination of GA+MG132 or GA+MG262 resulted in higher levels of ubiquitinated proteins and greater proteasome inhibition than each treatment alone (Figure 1A, lanes 4 and 6).

To further study the proteasome-inhibitory effect of GA, we transfected SH-SY5Y cells with a GFPu plasmid, a surrogate proteasome substrate. We found that GA treatment caused accumulation of both GFP and ubiquitinated proteins dose dependently (Figure 1C), confirming that GA is able to inhibit the cellular proteasome activity.

To determine whether GA is a direct proteasome inhibitor, an *in vitro* peptidase assay using an AMC fluorescence proteasome substrate was performed. GA at up to 5 μ M failed to inhibit the chymotrypsin (CT)-like activity of the purified 20S proteasome (Figure 1D). Only at 10–50 μ M doses, GA exhibited a partial inhibition (IC_{50} \sim 25 μ M, Figure 1D). These results demonstrated that GA itself is not a potent proteasome inhibitor. Consistently, the computational modeling studies predict that the GA metabolite MT1, but not GA and MT2, has the potential to interact with and inhibit the proteasomal β 5 chymotryptic subunit (Figure S1; see Extended Results).

MT1 and CYP2E1 Are Responsible for GA-Induced Proteasome Inhibition in Tumor Cells

To provide experimental evidence for MT1 as a direct proteasome inhibitor, MT1 was chemically synthesized and purified, and its effect on the CT-like activity of purified 20S proteasome was determined. As shown in Figure 2A, MT1 inhibited the purified 20S proteasomal CT-like activity with IC_{50} value of \sim 0.5 μ M, while in a sharp contrast, GA was inactive at up to 2.5 μ M (IC_{50} \sim 25 μ M, Figure 1D).

We then determined which isotype of CYP enzymes is responsible for metabolizing GA to MT1 and whether inhibition of this CYP enzyme could mitigate GA-induced proteasome inhibition by using a cell-based peptidase assay. We tested inhibitors of various CYP enzymes for their effects on GA-induced decrease in proteasome activities. We found that the inhibitors of CYP2D6 (Quinidine/Qui), CYP2C9 (sulfaphenazole/Sul), and CYP3A4 (ketocozazole/Ket) did not alter GA-induced proteasome inhibition in K562 cells (Figure 2B). However, diethyldithiocarbamate (DDC), a CYP2E1 inhibitor, dramatically rescued GA-induced

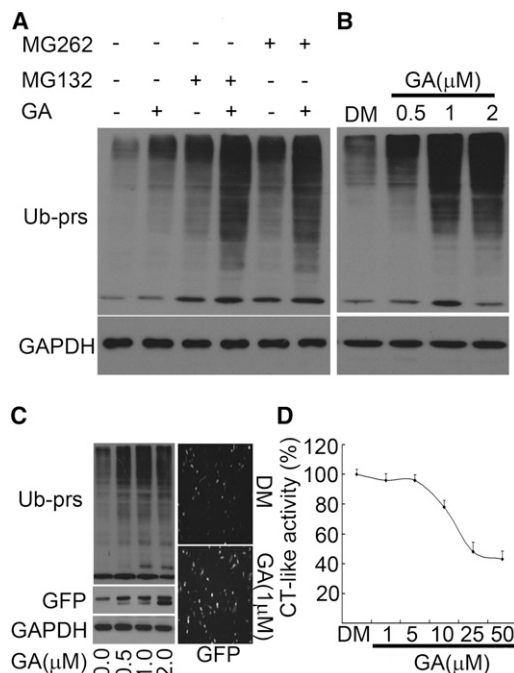


Figure 1. GA Indirectly Inhibits Proteasome Function

(A) GA enhanced ubiquitinated protein accumulation by MG132 and MG262 in human leukemic K562 cancer cells. K562 cells were treated with GA (0.5 μ M) for 12 hr in the absence or presence of proteasome inhibitors (MG132: 0.5 μ M; MG262: 0.025 μ M), followed by western blotting for total protein ubiquitination. GAPDH was used as a loading control. The western images were representatives from at least three independent experiments.

(B) GA dose dependently accumulated ubiquitinated proteins in K562 cells. K562 cells were exposed to either DMSO (DM) or GA for 12 hr, and ubiquitinated proteins and GAPDH were assayed as described in (A).

(C) GA induced the accumulation of GFPu and ubiquitinated proteins in GFPu-5Y cells. GFPu-5Y cells were treated with GA as indicated for 9 hr, and GFP expression was detected by an inverted epifluorescence microscope or western blotting.

(D) GA at 5 μ M or lower doses had no effect on 20S proteasome peptidase activities. Purified 20S proteasomes were treated with GA at the indicated doses in a Tris reaction system (pH 7.4). The CT-like peptidase activity was measured using specific synthetic fluorogenic substrates. Mean \pm SD (n = 3). See also Figures S1 and S2.

proteasome inhibition (Figure 2B), suggesting that CYP2E1 may be responsible for metabolizing GA into MT1. Indeed, DDC rescued GA-induced proteasome inhibition in K562 cells in a dose-dependent manner (Figure 2D), and such rescuing ability could be neutralized by increased concentrations of GA (Figure 2C). We have also noticed that GA only slightly inhibits the proteasomal caspase-like activity and dose not have any effect on the proteasomal trypsin-like activity (Figure S2), indicating that GA (or MT1) selectively inhibits cellular proteasomal CT-like activity. Furthermore, DDC was also able to suppress GA-induced proteasome inhibition in Jurkat T, P388, and HepG2 cells (Figures 2E and 2F; Figure S3).

To further validate the involvement of CYP2E1, we used small interfering RNA (siRNA) technology to silence intracellular CYP2E1, which should mimic the effect of its inhibitor DDC. siRNAs 1 and 2, but not 3 after transfection for 48 hr (Figure 2G)

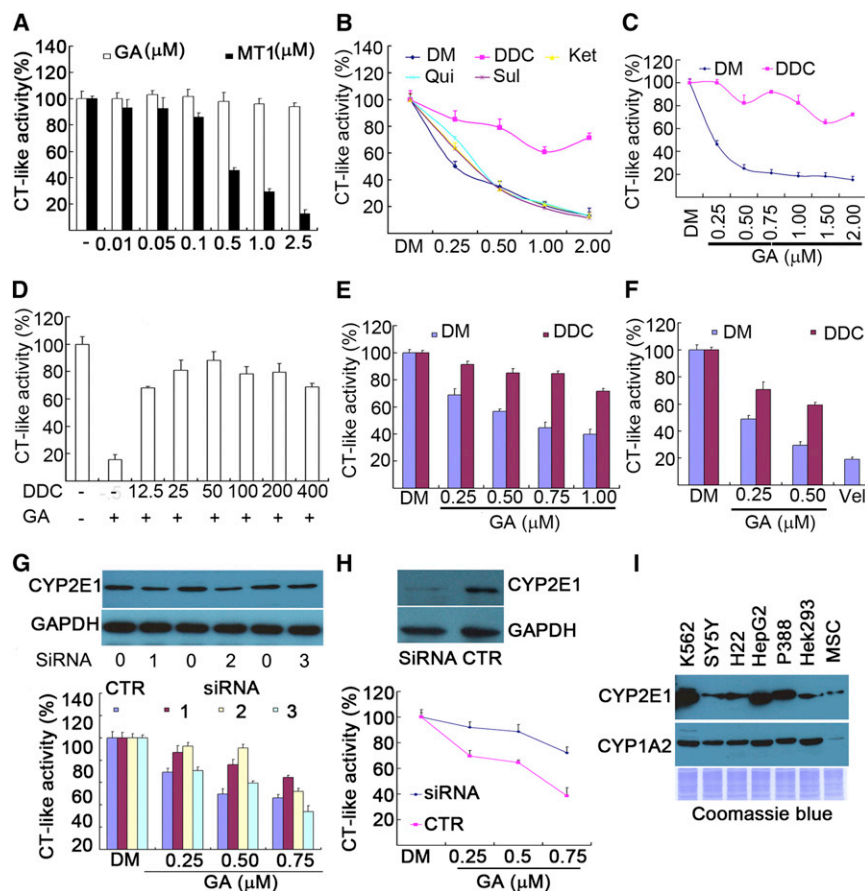


Figure 2. MT1 Directly Inhibits Proteasome Peptidase Activity and DDC or CYP2E1 siRNA Partially Disrupts GA-Mediated Proteasome Inhibition

(A) MT1 dose dependently inhibited 20S CT-like activity. 20S proteasome was treated with different doses of MT1 and GA, and CT-like activity was detected as in Figure 1D. Mean \pm SD (n = 3).

(B) The effects of P450 inhibitors on CT-like activities in cultured cells. K562 cells were exposed to P450 inhibitors (DDC, Ket, Qui, and Sul) for 6 hr, and then cell-based CT-like activity was detected. Mean \pm SD (n = 3).

(C) DDC partially reversed CT-like activity decrease induced by GA. K562 cells were incubated with GA in the presence of DDC (100 μ M) for 6 hr, and CT-like activities are shown. Mean \pm SD (n = 3).

(D) DDC reversed GA-induced proteasome inhibition in a dose-dependent manner. K562 cells were treated with various doses of DDC in the presence of GA (1 μ M) for 6 hr, and CT-like activity was assayed. Mean \pm SD (n = 3).

(E and F) DDC (100 μ M) partially reversed GA-induced proteasome inhibition in Jurkat and P388 cancer cells. As treated in (C), Jurkat cells and P388 cells were used for CT-like activity assay. Vel was used as a positive control. Mean \pm SD (n = 3).

(G and H) CYP2E1 siRNA partially silenced CYP2E1 expression and reversed proteasome inhibition. HepG2 cells were transfected with three CYP2E1-siRNA by using lipofectine 2000 agent for 48 hr, and western blotting was performed to detect the CYP2E1 protein level (#1 and #2 were effective, G, upper). At 48 hr transfection time point, various doses of GA

were added, and CT-like activity was assessed after 6 hr treatment (G, lower). As in (G), HepG2 cells were transfected with CYP2E1-siRNA (#2) for 72 hr, and CYP2E1 (upper) and CT-like activity (lower) were detected (H). Mean \pm SD (n = 3).

(I) CYP2E1 and CYP1A2 protein distribution in cancer cell lines by western blot. Human mesenchymal stem cells were used as control. Protein loading was detected by Coomassie blue.

See also Figures S3 and S4.

or siRNA 2 transfection for 72 hr (Figure 2H), were able to partially decrease the CYP2E1 protein in human HepG2 cells, associated with decreased levels of CT-like activity inhibition by GA. We further compared the CYP2E1 and CYP1A2 protein level in some of the cell lines by using human mesenchymal stem cell (hMSC) as a control. It was found that K562, P388, and HepG2 cancer cells have a higher level of CYP2E1 than other cells including normal cell (hMSC), while all the cell lines except hMSC have the similar level of CYP1A2 (Figure 2I).

It has been reported that proteasome inhibition could induce typical gene expression profile in many cancer cell lines. We then compared the gene expression profiles between GA and Vel treatment. We found that GA and Vel yielded not only a similar gene expression profile but also the similar proteasome inhibition-specific genes (Figure S4; see Extended Results).

Proteasome Inhibition Induced by the Metabolite Produced by CYP2E1 Is Required for GA's Cytotoxicity

We next determined whether proteasome inhibition contributes to GA-induced cytotoxicity. We found that inhibition of

CYP2E1 by DDC not only partially rescued GA-induced proteasome inhibition (Figure 2), but also inhibited GA-induced cell death in P388 and K562 cells (Figures 3A–3G). Exposing P388 cells to 1 μ M of GA for 6 hr in the absence or presence of DDC resulted in \sim 60% and \sim 20% cell death, respectively (Figures 3A and 3B). Furthermore, GA induced cleavage of PARP and activation of caspase-9 (but not caspase-8) and caspase-3 dose dependently, which was completely inhibited by DDC (Figures 3C).

The result that inhibition of CYP2E1 suppressed GA-induced proteasome inhibition (Figure 2) suggests that MT2 has no proteasome-inhibitory activity. Since it is known that CYP1A2 is the major P450 that is responsible for metabolizing GA to MT2, one would expect that inhibition of CYP1A2 would lead to no production of MT2 from GA, which would result in presumably increased levels of MT1 and consequent proteasome inhibition. It has been shown that α -naphthoflavone (ANF) at a concentration of 12.5–100 μ M is a strong CYP1A2 inhibitor (Liu et al., 2006). In K562 cells, GA+ANF treatment produced higher levels of ubiquitinated proteins than each treatment alone (Figure 3D).

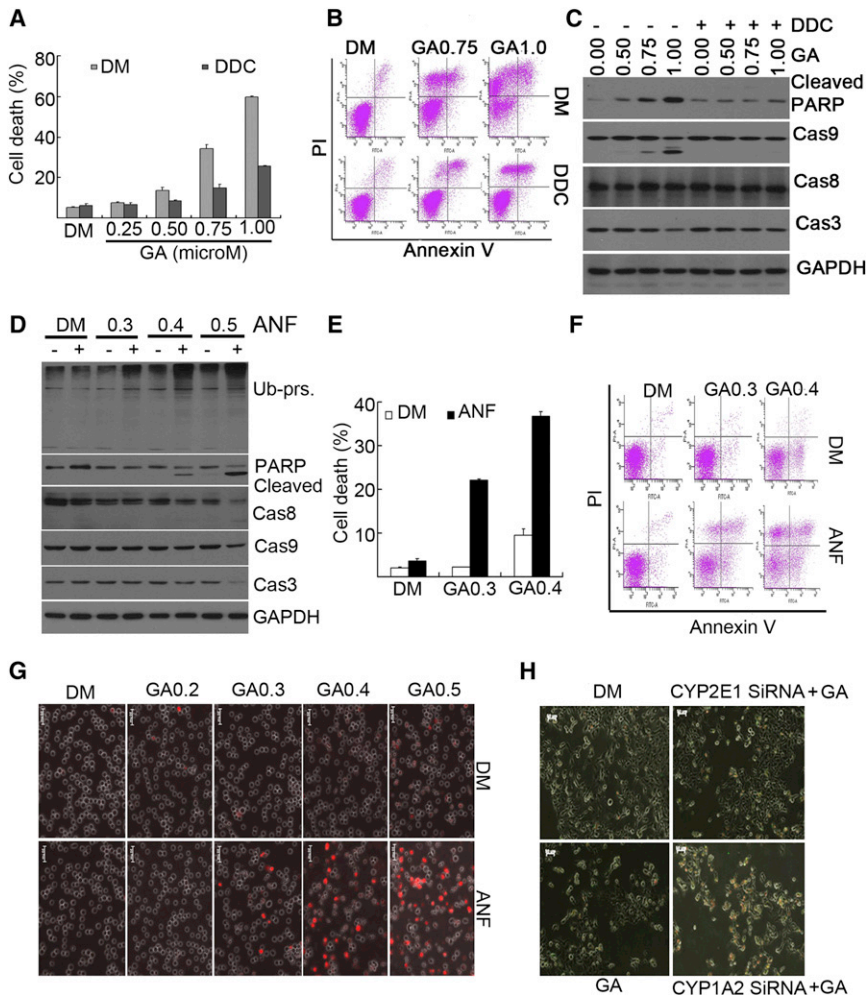


Figure 3. DDC Treatment or CYP2E1 Silencing Partially Reversed while Inhibiting CYP1A2 Enhanced GA-Induced Cell Death in Cultured Cancer Cells

(A and B) DDC partially reversed GA-induced cell death in P388 cells. P388 cells were treated with GA for 6 hr in the presence of DDC (100 μ M), and cell death was detected by Annexin V and PI staining with a flow cytometer. Cell death data were summarized (A) ($n = 3$), and typical images were shown (B).

(C) Similar to (B), DDC (100 μ M) partially rescued GA-induced caspase activation and PARP cleavage by western blotting using specific antibodies as indicated.

(D) α -Naphthoflavone (ANF) enhanced GA-induced caspase activation and PARP cleavage. K562 cells were treated with GA for 9 hr in the presence of ANF (25 μ M), followed by western blotting using specific antibodies.

(E and F) ANF enhanced GA-induced cell death by flow cytometry. Similar to (D), cell death was assayed and summarized (E), and representative flow images were shown (F).

(G) ANF enhanced GA-induced cell death by PI staining in living cells. K562 cells were treated with GA, with or without ANF (25 μ M), cell death was detected by PI staining in living cells. Representative images at 24 hr were shown. Scale bar = 50 μ m.

(H) Silencing CYP2E1 partially reversed GA-induced cell death while silencing CYP1A2 enhanced GA-induced cell death. HepG2 cells were transfected with CYP2E1-siRNA and CYP1A2-siRNA for 48 hr, and then cells were treated with 0.75 μ M of GA for 12 hr, and cell death was stained with Annexin/PI double staining in situ and recorded under an inverted fluorescence microscope.

See also Figures S5, S6, and S7.

ANF alone has no effect on the levels of the proteasome activity and ubiquitinated proteins. Furthermore, GA+ANF treatment resulted in higher levels of apoptotic cell death than each treatment alone, as measured by increased PARP cleavage and caspase cleavage/activation (Figure 3D). ANF also enhanced GA-induced cell death with propidium iodide (PI) staining in living cells (Figure 3G), and with annexin V/PI double staining by flow cytometry (Figures 3E and 3F). We have also found that GA-induced proteasome inhibition and cytotoxicity could be partially reversed by DDC-mediated CYP2E1 inhibition in myeloma cancer cells (Figure S5; see Extended Results).

To further confirm that the cell death induction by GA is due to CYP2E1, CYP2E1- and CYP1A2-siRNA were used to silence CYP2E1 or CYP1A2, respectively. We found that, similar to proteasome inhibition, silencing CYP2E1 partially rescued GA-induced cell death, whereas silencing CYP1A2 enhanced GA-induced cell death (Figure 3H; Figure S6). These results clearly showed that GA-induced cytotoxicity relies on its proteasome-inhibitory activity, which is mediated mainly by CYP2E1 and its metabolite MT1.

We also found that similar to Vel, GA was able to induce endoplasmic reticulum (ER) stress, as measured by increased levels

of ER-stress-related proteins, CHOP, Bip, PERK, and IRE-1 α (Figure S7). The profiles of other ER-related proteins PDI, Ero-1 α , and calnexin were also similar between GA and Vel treatment. GA at 0.75 μ M yielded the similar effect on ER stress responses and PARP cleavage to 50 nM dose of Vel in HepG2 cells (Figure S7). These results demonstrated that, similar to Vel, GA induced the ER stress responses that are associated with proteasome inhibition-mediated cytotoxicity.

GA Treatment Increases the Survival of P388-Bearing Mice and Inhibits H22 Tumor Growth and Proteasome Function In Vivo

We next determined the anticancer effect of GA in vivo by recording the cumulative survival of mice bearing P388 tumors. Male KMF mice were inoculated by intraperitoneal (i.p.) injection with P388 cells and then started i.p. bolus injections of drug vehicle or 1.5 mg/kg GA for 7 consecutive days, followed by monitoring survival for the next 60 days (Figure 4A). We found that all the mice in the vehicle-treated group died within 23 days. In a sharp contrast, only two mice in the GA-treated group died on day 20 and day 33, respectively, and all the others survived to the end of the experiment (Figure 4A).

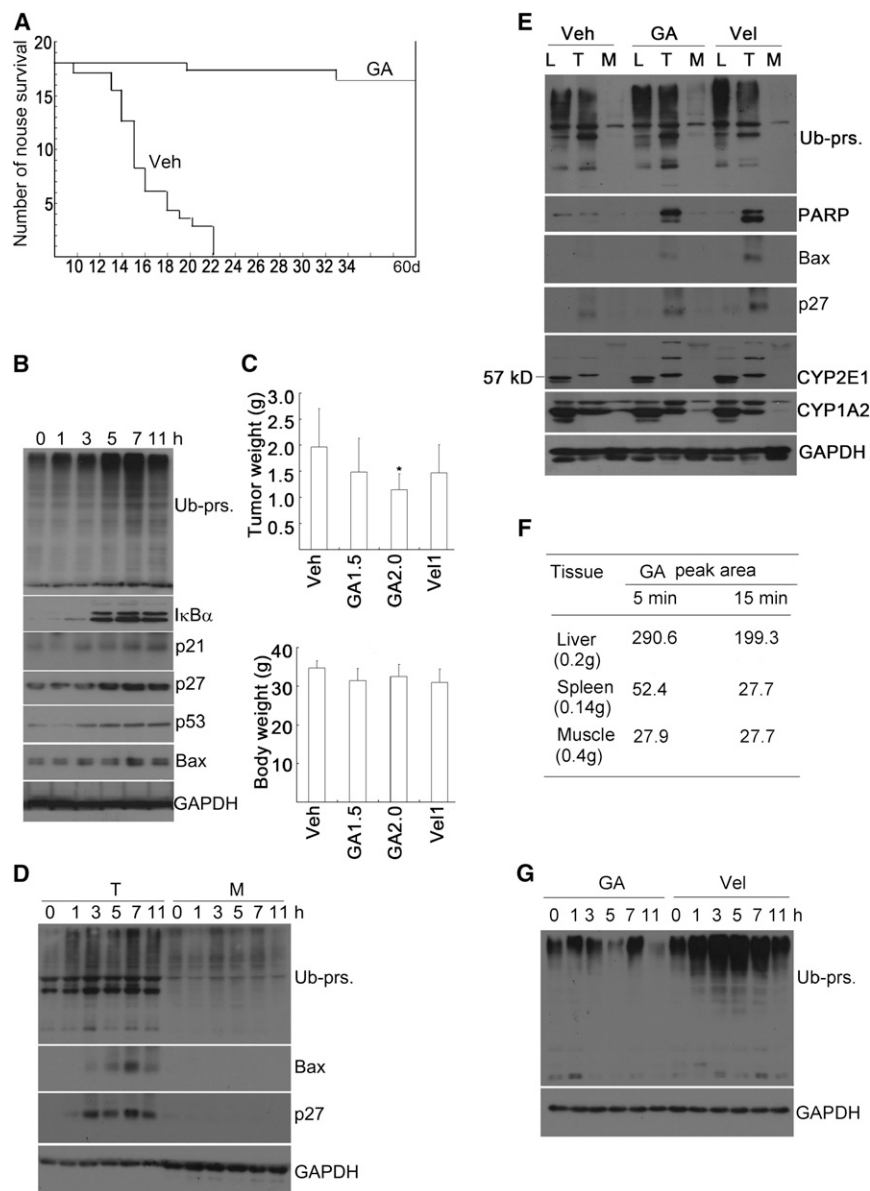


Figure 4. GA Prolongs Survival of Ascities Bearing P388 Leukemic Cells and Suppresses Solid Tumor Growth In Vivo

(A) GA's effect on cumulative survival in KMF mice bearing P388 leukemic cells. Mice bearing P388 cells were treated with i.p. bolus injections of either vehicle (Veh) or 1.5 mg/kg/day GA for consecutive 7 days. The mice were then kept for 60 days.

(B) GA inhibited proteasome proteolytic function in vivo. Mice were inoculated with P388 cells for 5 days, and then GA (2 mg/kg) was i.p. injected once. At 1, 3, 5, 7, and 11 hr after GA injection, ascities were collected for western blot assay.

(C) GA inhibited tumor growth in vivo. H22 allografts in male KMF mice were treated with either vehicle or GA at 1.5, 2.0 mg/kg, or 1 mg/kg of Vel (ten mice each group) for consecutive 7 days. Two days later after that, the mice were sacrificed; body weight and the tumor tissues were weighed. Mean \pm SD, * $p < 0.0001$.

(D) GA inhibited proteasome proteolytic function in solid tumor in vivo. Mice bearing mouse H22 tumor were i.p. treated with GA (2 mg/kg) once; at 1, 3, 5, 7, and 11 hr after GA injection, tumor (T) and muscle tissues (M) were collected for western blot assay.

(E) GA and Vel only induced PARP cleavage in tumor tissues in vivo. As in (D), three mice bearing H22 tumor were i.p. injected with GA (3 mg/kg) once, and 12 hr later after injection, tumor, muscle, and liver tissues (L) were collected for detecting ubiquitinated protein, p27, Bax, PARP, CYP2E1, and CYP1A2 by western blot. One representative western image was shown.

(F) GA relative content in mouse tissues. KMF mice were i.v. injected with GA (8 mg/kg) for 5 or 15 min, and GA content was detected by high-performance liquid chromatography assay. The peak area of GA in various tissues was calculated (average of three repeats).

(G) Accumulation of ubiquitinated proteins in spleen tissues. Mice were i.p. injected with GA (2 mg/kg) or Vel (1 mg/kg) as in (D), and ubiquitinated proteins in spleen tissues were detected by western blot.

To confirm whether GA inhibits the proteasome function in vivo, dynamic changes of the endogenous proteasome substrates were assessed. A separate cohort of male KMF mice was inoculated with P388 cells. Five days later, mice bearing P388 ascities were i.p. injected with 2 mg/kg of GA. At different time points, ascities were collected for western blotting assay. It was found that the proteasome substrate proteins, including IκBα, p21, p27, p53, and Bax as well as ubiquitinated proteins all accumulated in a time-dependent manner (Figure 4B), indicative of rapid proteasome inhibition after GA injection. We also tried to measure the CT-like activity in these p388 cancer cells. However, like in other cultured cells, CT-like activity inhibition could be detected only by cell-based activity assay but not by in vitro assay using AMC-conjugated proteasome substrate after GA treatment (data not shown). These results

suggest that the binding of metabolite of GA to proteasome β5 subunit is unstable or transient during protein extraction process, indicating that GA-induced proteasome inhibition is mostly reversible.

We then determined the antitumor effect of GA in a solid tumor model in vivo. Male KMF mice were inoculated subcutaneously (s.c.) in the left armpit with H22 cells, followed by treatment with GA at 1.5 and 2.0 mg/kg for 7 consecutive days, or Vel at 1 mg/kg every 3 days. Ten days after the inoculation, all the mice were sacrificed, and the tumors were weighed. As shown in Figure 4C (upper), tumor weight in the vehicle-treated group reached $\sim 1,900$ mg on average, while tumor weight from groups treated with 1.5 or 2.0 mg/kg GA was $\sim 1,400$ and $\sim 1,100$ mg, respectively, demonstrating $\sim 24\%$ and $\sim 45\%$ inhibition. At both doses, GA did not affect the body weight at the end of

the experiment (Figure 4C, lower). At 1 mg/kg, Vel could inhibit ~23% of the growth of H22 allograft close to 1.5 mg/kg GA treatment, and the body weight in Vel-treated mice was similar to the control mice.

To investigate whether GA could selectively inhibit the proteasome function in solid tumor tissues over normal tissues, KMF mice bearing H22 tumor were i.p. injected with 2 mg/kg of GA. At different time points after GA injection, proteasome substrate proteins p27 and Bax as well as ubiquitinated proteins were found to be accumulated in tumor tissues but not in muscle tissues (Figure 4D). We further measured and compared the levels of proteasome inhibition, PARP cleavage, and CYP2E1/CYP1A2 in normal and tumor tissues in mice bearing H22 tumor after i.p. injection with either GA (3 mg/kg) or Vel (1 mg/kg) for 12 hr. As shown in Figure 4E, accumulation of proteasome substrate proteins p27 and Bax could be detected in tumor tissues but not muscle tissues, although ubiquitinated proteins were found to be increased in both tumors and liver tissues but not normal muscle tissues (Figure 4E) after GA and Vel treatment. Furthermore, GA and Vel selectively induced PARP cleavage only in tumor tissues but not in normal muscle and liver tissues (Figure 4E), indicating that cancer cells are more sensitive to proteasome inhibition than normal cells. Importantly, after treatment of GA and Vel increased expression mainly in CYP2E1 (and slightly in CYP1A2 protein) was found in tumors, but not in normal muscle tissues (Figure 4E). The increased CYP2E1 protein should be able to enhance the effects of GA. These data demonstrate that GA treatment inhibits H22 solid tumor growth and significantly improves animal survival in leukemic mice, associated with proteasome inhibition at early hours.

To further test whether GA is a tissue-specific proteasome inhibitor in vivo, we detected GA distribution in some of the relevant normal tissues after GA injection in mice. It was found that GA could be detected in liver, muscle, and spleen tissues (Figure 4F), consistent to a previous report (Hao et al., 2007). GA relative content is 0.69 in rat spleen tissue and 1.15 in liver tissue after GA intravenous (i.v.) injection for 45 min (spleen:liver: ~60%) (Hao et al., 2007). When tested in mice, Vel relative content is ~3,100 in spleen tissue and ~4,500 in liver tissue after i.v. injection of Vel for 60 min (spleen:liver: ~68%) (Adams et al., 1999). We therefore further detected the proteasome substrate accumulation in spleen tissues after treatment with GA or Vel. We found that Vel, but not GA, could dramatically accumulate ubiquitinated proteins (Figure 4G). Other proteasome substrates like p27 and Bax were not detected (data not shown). Therefore, although low levels of GA were detectable in spleen, it did not cause proteasome inhibition in this organ, unlike Vel. These results have further demonstrated that GA induces tissue-specific proteasome inhibition, compared to Vel.

The Reduced Form of GA Fails to Induce Proteasome Inhibition and Cytotoxicity

To investigate the requirement of the C₉-C₁₀ double bond of GA for proteasome inhibition, C₉-C₁₀-disrupted GA (GA~), a reduced form of GA, was chemically synthesized (Figure 5A). K562 cells were treated with various doses of GA and GA~ for

6 hr. Cell-based CT-like activity was detected. It was found that GA~ lost its ability to inhibit proteasome activity at a dose up to 5 μM, and the IC₅₀ of GA~ for proteasome inhibition is around 10 μM, 40-fold higher than the IC₅₀ of GA (0.25 μM, Figure 5B). Accordingly, GA dose dependently inhibited cell viability after 24 or 48 hr treatment in K562 cells, while GA~ at <2 μM did not exert any effect on cell viability (Figure 5C); 0.75 μM of GA induced typical cell death, while GA~ at up to 5 μM did not induce any cell death after 18 hr (Figure 5D). Further studies in K562 cells found that GA induced PARP cleavage and ubiquitinated protein accumulation, while GA~ did not (Figure 5E). Similar results were found in a myeloma cell line NCI-H929: at 1 μM or lower doses, GA~ did not inhibit CT-like activity, while GA inhibited CT-like activity with an IC₅₀ between 0.25~0.5 μM (Figure 5F). Consistent to what was observed in K562 cells, GA~ at <1 μM did not exert any effect on cell viability (Figure 5G) and at <5 μM did not affect cell death either (Figure 5H), while GA at <1 μM dose dependently inhibited cell viability and induced cell death in NCI-H929 cells. These results clearly demonstrated that GA-induced cytotoxicity and cell death definitely depend on the existence of C₉-C₁₀ double bond, which is required for its mediated proteasome inhibition.

GA Does Not Decrease Lymphocyte Survival in CYP2E1-Deficient Peripheral Blood Cells In Vitro and In Vivo

To further study this importance of CYP2E1 in mediating GA-induced proteasome inhibition and cytotoxicity, the red blood cells were collected after 24, 48, and 72 hr from mice treated with either GA (3 mg/kg, i.p.) or Vel (1 mg/kg, i.p.). GA 3 mg/kg is an effective dose of anticancer therapy (Yi et al., 2008). As expected, only Vel but not GA at the tested doses inhibits the proteasomal CT-like activity in the peripheral blood cells (Figure 6A) by in vitro peptidase assay. We further detected the peptidase activity in peripheral blood cells by using cell-based CT-like activity assay and found that GA did not inhibit CT-like activity in whole blood cell culture either (Figure 6B). These data demonstrate that GA could inhibit the proteasome function in a cell-specific manner.

Using a whole blood cell culture system, we next compared the effects of GA and Vel on the survival of blood cells. We first screened the optimal dose of GA and Vel yielding the similar effect on cell viability in cancer cells. It was found that in HepG2 cells, 500 nM of GA yielded the similar effect on cell viability to 50 nM of Vel (data not shown). In the next peripheral blood experiment, the relative high dose of GA and Vel was used. As expected, GA at 1 μM did not show any effects on the survival of blood cells during 7 days of culture (Figure 6C), while Vel at 0.1 or 0.5 μM dose inhibited white blood cell and lymphocyte survival as expected (Figure 6D). These results show that GA led to cell-specific proteasome inhibition.

One of the most important side effects of chemotherapy is the inhibition of the hemopoietic system (Richardson et al., 2005). To further confirm whether therapeutic dose of GA could affect white blood cell number, the CYP2E1 and CYP1A2 protein distribution in mouse and human bone marrow cells were compared with cancer cell lines (Figure 6E). In mouse bone

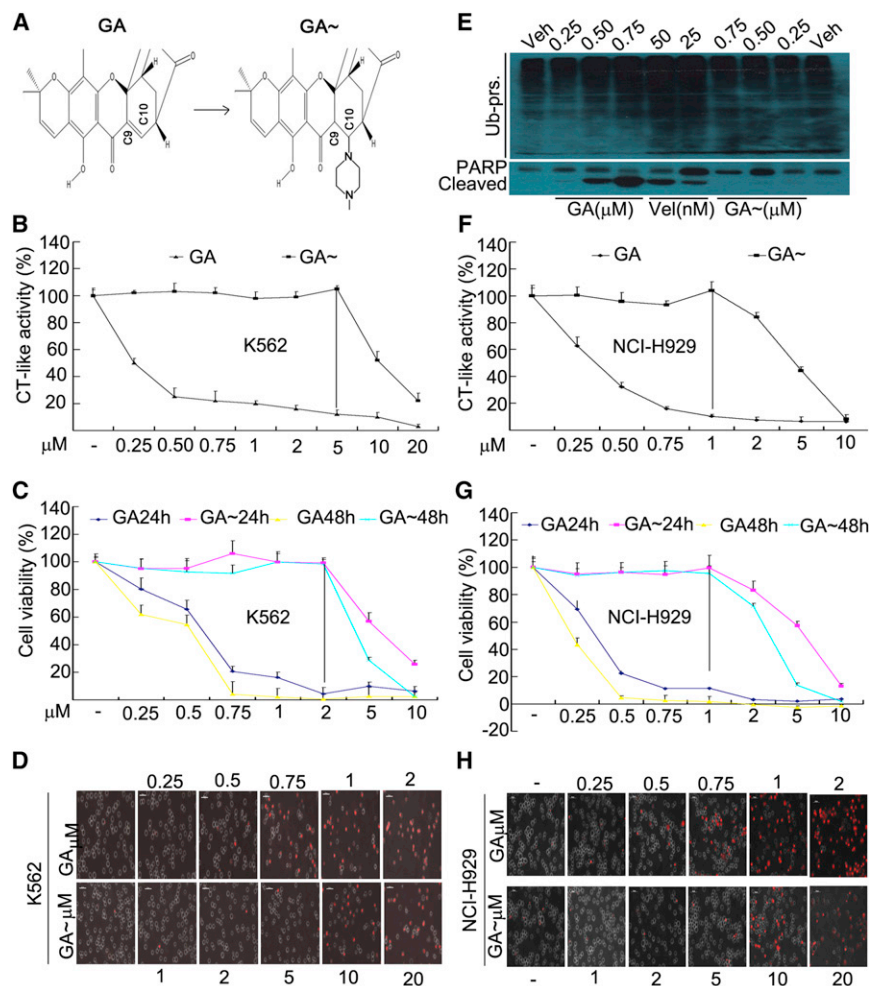


Figure 5. C₉-C₁₀-Disrupted GA Fails to Induce Proteasome Inhibition, Proliferation Inhibition, and Cell Death

(A) Chemical structure of GA and GA~. C₉-C₁₀ double bond was disrupted by adding a piperazine to C₁₀.

(B) GA~ failed to inhibit CT-like activity in K562 cells. K562 cells were treated with GA and GA~ for 6 hr, and CT-like activity in living cells was detected as described above. Mean ± SD (n = 3).

(C) GA~ failed to inhibit cancer cell viability in K562 cells. K562 cells were treated with GA or GA~ for 24 or 48 hr, and cell viability was detected by MTS assay. Mean ± SD (n = 3).

(D) GA~ lost its ability to induce cell death in K562 cells. K562 cells were treated with GA or GA~, PI was added to the cultured cells after 6 hr treatment, and PI-positive staining was monitored under an inverted microscope and typical images at 18 hr time point were shown.

(E) GA~ failed to induce accumulation of ubiquitinated proteins and PARP cleavage. K562 cells were treated with various doses of GA or GA~ for 12 hr, and cells were collected. PARP cleavage and ubiquitinated proteins were detected by western blot.

(F) GA~ failed to inhibit CT-like activity in NCI-H929 cells. NCI-H929 cells were treated as in (C), and CT-like activity was detected. Mean ± SD (n = 3).

(G) GA~ failed to inhibit cancer cell viability in NCI-H929 cancer cells. NCI-H929 cancer cells were treated as in (C), and cell viability was detected. Mean ± SD (n = 3).

(H) GA~ lost its ability to induce cell death in NCI-H929 cells. NCI-H929 cells were treated and cell death was detected as in (D). PI-positive staining was monitored under an inverted microscope, and typical images at 6 hr time point were shown.

marrow cells, CYP1A2 was highly, while CYP2E1 was weakly, expressed compared to the cancer cells (Figure 6E, left). It was further found that CYP2E1 and CYP1A2 proteins were weakly expressed in normal human bone marrow cells compared with the bone marrow cells from leukemic patients (Figure 6E, right). These results indicated that both normal mouse and human bone marrow cells weakly express CYP2E1 protein, indicating an inability for the bone marrow cells to metabolize GA. Second, Balb/c mice were treated with both GA (4 mg/kg) or Vel (0.5, 1 mg/kg) for 2 weeks, and then peripheral white blood cells were counted. GA at 4 mg/kg once every other day is effective anticancer therapy (Guo et al., 2006) and 0.5 mg/kg or 1 mg/kg dose of Vel is also effective dose of anticancer therapy. GA was i.v. injected once every other day and Vel was i.v. injected once every 3 days. It was found that therapeutic dose of GA (4 mg/kg) did not affect either body weight or peripheral white blood cells, and Vel (0.5 mg/kg) did not affect these changes either, while Vel at 1 mg/kg dose did not affect body weight but dramatically decreased the peripheral white blood cell number (Figure 6F). These results demonstrated that GA did not affect cell survival in CYP2E1-deficient cells either in vitro and in vivo.

GA Induces More Cytotoxicity and Proteasome Inhibition in Cancer Cells from Leukemic Patients Than in Human Peripheral Mononuclear Cells

We have confirmed that GA induced cytotoxicity and proteasome inhibition in cancer cell lines and in vivo; next, we further compared the effects of GA on cytotoxicity and proteasome inhibition in cancer cells obtained from ten leukemia patients (five AML-M5, three AML-M2, one ALL, one CLL) and in peripheral mononuclear cells from six normal volunteers. It was found that GA at all the doses more dramatically decreased cell viability in leukemic cells than in normal cells while the difference of Vel-mediated cytotoxicity in leukemic cells and normal cells is not as high as GA (Figure 7A); GA, similar to Vel, also induced leukemic cancer cell death (Figures 7B–7D). GA 0.75 μM yielded the similar effects on cell viability and cell death induction to 100 nM Vel. To determine the levels of proteasome inhibition, ubiquitinated proteins were detected by western blot. As shown in Figures 7E and 7F, 50 nM Vel markedly induced accumulation of ubiquitinated proteins and PARP cleavage in normal mononuclear cells while GA only slightly induced these changes compared to Vel; but in leukemic cancer cells, GA at all the three doses markedly induced both ubiquitinated protein

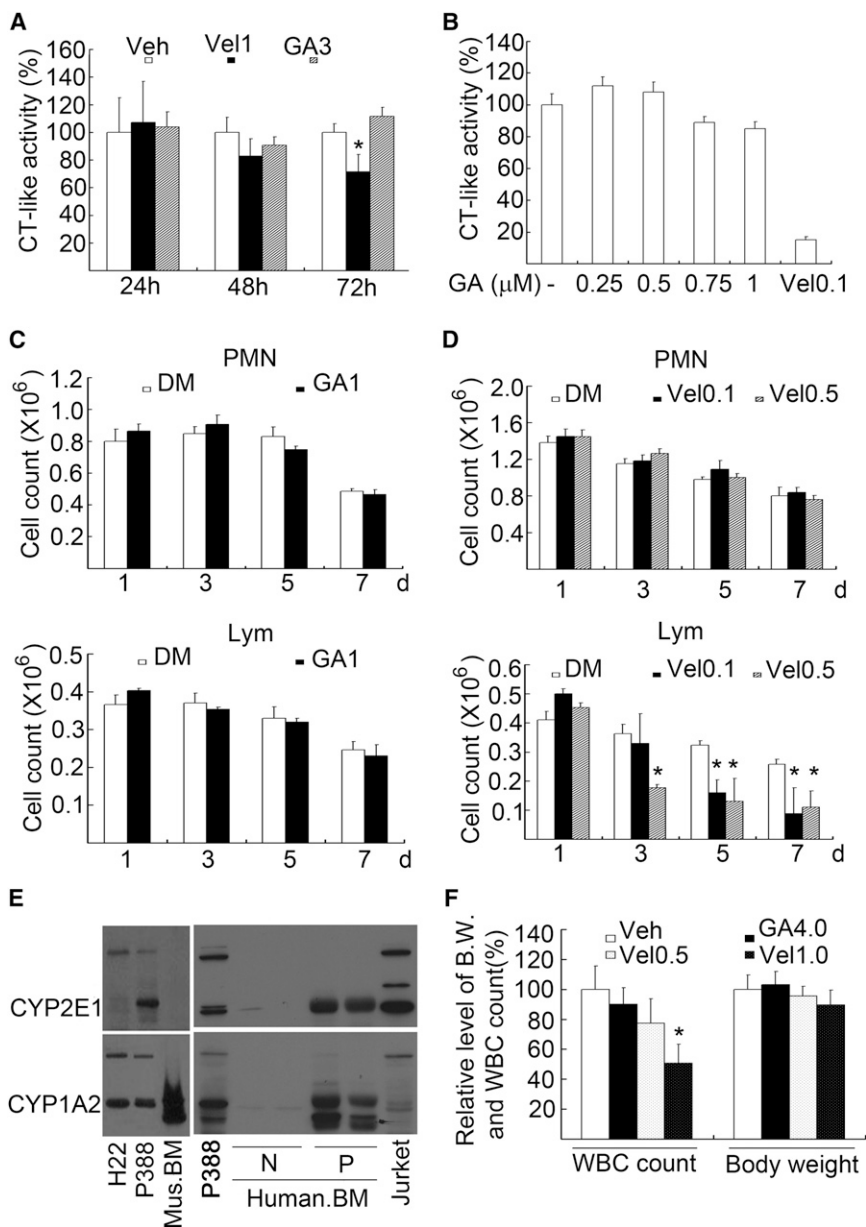


Figure 6. GA Does Not Inhibit White Blood Cell Survival In Vitro and In Vivo

(A) GA did not inhibit proteasome CT-like activity of red blood cells in vivo. Balb/c mice (n = 3) were i.p. injected with Vel (1 mg/kg) or GA (3 mg/kg) once, and red blood cells were collected for CT-like activity assay after 24, 48, and 72 hr. Veh: vehicle. Mean ± SD.

(B) GA did not affect CT-like activity in cultured blood cells. Human peripheral whole blood was exposed to GA for 6 hr, and CT-like activity was assayed in living cells by using a cell-based CT-like assay substrate. The relative CT-like activity was shown (n = 3). 100 nM of Vel was used as a positive control.

(C) GA did not inhibit lymphocyte survival in vitro. Human peripheral whole blood was cultured in the absence or presence of 1 μM GA for 1, 3, 5, and 7 days. The cell count data of polymorphonuclear (PMN) cells and lymphocytes in DMSO (DM) or GA-treated group were shown, respectively. Mean ± SD (n = 3).

(D) As in (C), the cells were treated with Vel (0.1, 0.5 μM) instead of GA, and the cell count data were shown, respectively. Mean ± SD (n = 3).

(E) CYP2E1 and CYP1A2 distribution in mouse and human bone marrow cells. CYP2E1 and CYP1A2 protein in mouse and human bone marrow cells (normal control and leukemic sample) were detected by western blot. Cancer cell lines as indicated were used as controls. CYP2E1 and CYP1A2 western images in mouse bone marrow were one representative of the three repeats. CYP2E1 and CYP1A2 in human bone marrow were repeated twice, and representative images were shown.

(F) Therapeutic dose of GA (4 mg/kg) did not decrease the white blood cell count in vivo. Balb/c mice were i.v. injected with GA (4 mg/kg) once every 2 days and Vel (0.5, 1.0 mg/kg) once every 3 days for a total of 14 days. Relative level of white blood cell count and body weight were summarized. Mean ± SD (n = 3). *p < 0.05, versus vehicle (Veh) control.

accumulation and PARP cleavage (Figures 7G and 7H). These results demonstrated that GA, compared to Vel, selectively induced proteasome inhibition and cytotoxicity in leukemic cancer cells.

DISCUSSION

GA Is Metabolized to a Potent Proteasome Inhibitor by P450 Enzyme in the Cell

In the current study, we report that GA inhibits activity of cellular 26S proteasome but not purified 20S proteasome, suggesting that GA is a proteasome inhibitor prodrug. Furthermore, we found that GA-induced proteasome inhibition is mediated by P450 enzyme. The proteasomal subunits β5, β2, and β1 in 20S

catalytic core are responsible for three main proteolytic activities of the proteasome, CT-like, trypsin-like, and caspase-like activities, respectively. A threonine residue at the N terminus (Thr1) of these subunits imparts the catalytic activity of the proteasome (Groll et al., 2005). The atom O^γ of Thr1 (Thr1 O^γ) is activated to be nucleophilic by proton shuttling from Thr1 O^γ to the proton acceptor Thr 1 N. Compounds with electrophilic functional groups are able to react with the nucleophilic Thr 1 O^γ, causing interference of the proteasomal activity. Consistently, in the computational modeling study, MT1 but not GA nor MT2 was docked to the proteasomal β5 subunit that was suitable for nucleophilic attack by Thr 1 of the β5 subunit (Figure S1). As expected, further studies confirmed that the C₉-C₁₀ double bond of GA is a prerequisite for GA-induced proteasome inhibition (Figure 5). It was also found that GA induced the similar ER stress responses (Figure S6) and yielded the similar gene

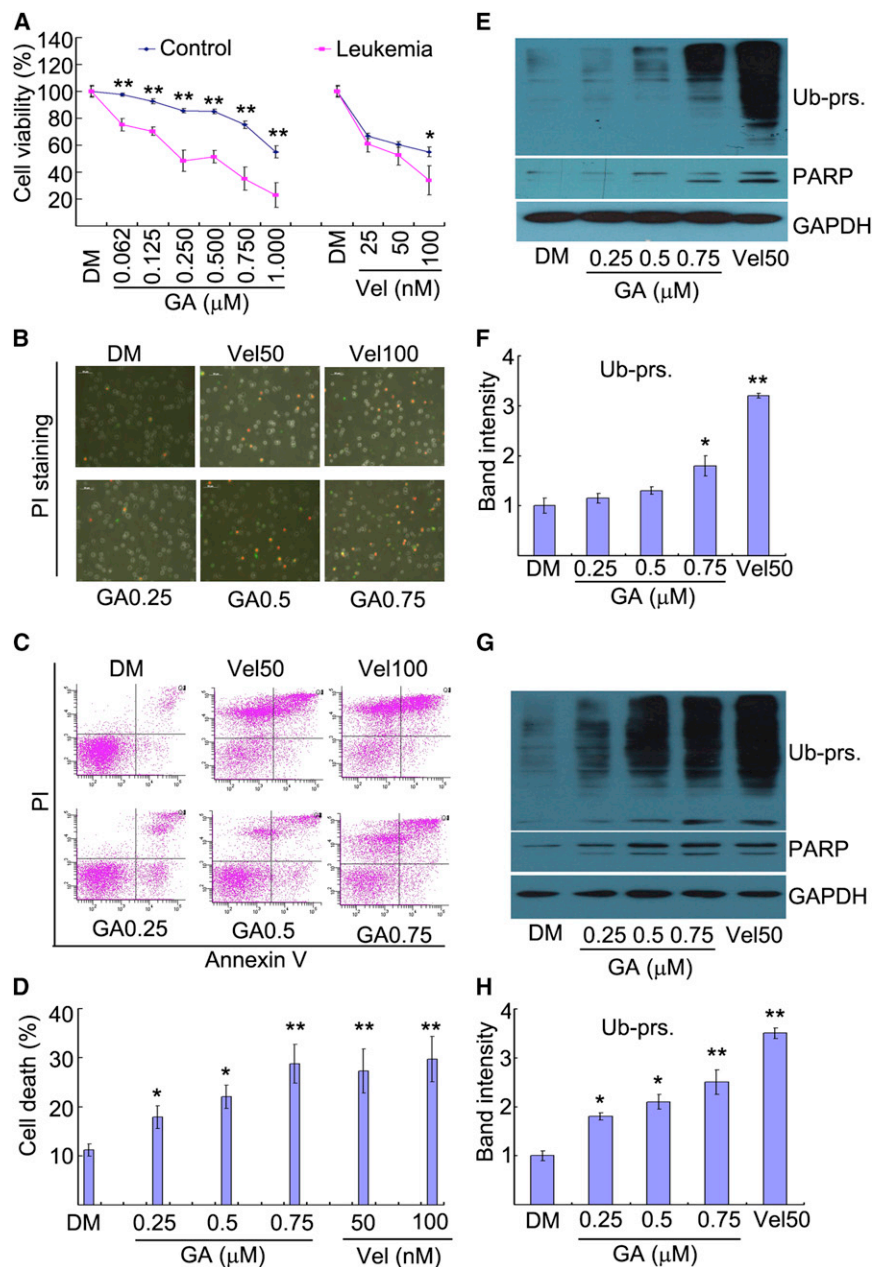


Figure 7. GA-Induced Cytotoxicity and Proteasome Inhibition in Cancer Cells from Patients with Leukemias

(A) GA dose dependently decreased leukemic cell viability. Mononuclear cells isolated from either patients or volunteers were treated with GA and Vel for 24 hr, and cell viability was detected by MTS assay. Control group: $n = 6$; Leukemia group: $n = 9$. * $p < 0.05$, ** $p < 0.01$, versus each dose of leukemia group.

(B–D) GA induced cell death in leukemic cancer cells. Leukemia cells were treated by three doses of GA and two doses of Vel for 24 hr, cells were labeled with PI and Annexin F-FITC, and the fluorescence was detected with flow cytometry or observed under a fluorescence microscope. Total samples from seven leukemia patients were detected for cell death assay. One representative morphological image is shown in (B) and flow image is in (C). Cell death data from seven patients by flow cytometry are shown in (D). Mean \pm SD ($n = 7$), * $p < 0.05$, ** $p < 0.01$, compared to the vehicle control.

(E–H) GA induced more ubiquitinated protein accumulation and PARP cleavage in leukemia cancer cells than in normal cells. Mononuclear cells were incubated with GA and Vel (50 nM) for 15 hr, and ubiquitinated protein and PARP were detected by western blot. GAPDH was used as a loading control. A representative western image from three repeats is shown in (E), and the band intensities of ubiquitinated proteins ($n = 3$) are summarized in (F) in normal mononuclear cells, while, in leukemia cancer cells, a representative western image from three repeats is shown in (G), and the band intensities of ubiquitinated proteins ($n = 3$) are summarized in (H). * $p < 0.05$, ** $p < 0.01$, versus vehicle control.

expression profile (Figure S4) to the specific proteasome inhibitor Vel. These results confirm that GA indirectly and potentially targets tumor proteasome in the cell.

Even though the metabolite MT1 could directly inhibit CT-like activity, we could not completely exclude the possibility for GA-induced metabolite MT1 to interact with the 19S proteasome mainly for two reasons: (1) MG132 at 0.5 μM and MG262 at 0.25 μM completely inhibit the proteasome CT-like activity, but these doses of agents and GA could still synergistically accumulate ubiquitinated proteins; (2) the optimal IC_{50} value of MT1 for 20S proteasome CT-like activity is around 0.5 μM , but the IC_{50} value in some of the leukemic cells was as low as 0.25 μM , indi-

cating that GA could possibly affect both 20S and 26S proteasome. We then determined whether proteasome inhibition is required for GA's cytotoxicity and anticancer activity. We found that blocking the CYP1A2 pathway enhanced, while blocking CYP2E1 pathway reversed GA-induced proteasome inhibition and cell death. Importantly the IC_{50} of GA for cancer cellular

GA at Therapeutic Dose Induces Cytotoxicity via Proteasome Inhibition

ubiquitinated protein accumulation in the absence of CYP2E1 in normal mononuclear cells (Choudhary et al., 2005). We could therefore not completely exclude other P450 enzymes besides CYP2E1 involved in the metabolism of GA to MT1.

proteasome activity is 0.25–0.75 μM , similar to its IC_{50} (0.5–1.5 μM) for cytotoxicity (Zhang et al., 2004). These data imply that proteasome inhibition is a prerequisite for GA-induced cell proliferation arrest and cell death. An early study reported that transferrin receptor is an important target of GA and the lowest IC_{50} for inhibiting transferrin receptor is $>2 \mu\text{M}$ (Pandey et al., 2007), but the IC_{50} of GA's cytotoxicity is $<1 \mu\text{M}$, mostly 0.5 μM in cancer cell lines (Zhang et al., 2004). Another reported important target is related to angiogenesis (Yi et al., 2008), but based on our data, leukemic cancer cells were more sensitive to GA compared to other nonleukemic cells, and GA significantly improved mouse survival bearing P388 ascities in which no angiogenesis exists.

Even though CYP2E1 inhibition by either chemical inhibitor DDC or siRNA could partially reverse GA-induced proteasome inhibition and cytotoxicity, we still could not completely exclude the off-target effect of GA on cell viability and cell death. Since the $\text{C}_9\text{-C}_{10}$ double bond of GA is responsible for GA-induced proteasome inhibition, we therefore synthesized a reduced form of GA by disrupting the $\text{C}_9\text{-C}_{10}$ double bond of GA. After disruption of this double bond, as expected, GA~ lost its ability to inhibit proteasome activity within 5 μM dose. Accordingly, GA~ at $<5 \mu\text{M}$ did not induce any cell death, indicating that proteasome inhibition is required for GA-induced cell death. The most important is that both in NCI-H929 and K562 cancer cells, GA~ at <1 or 2 μM doses did not affect either the cell viability or cell proliferation, indicating that proteasome inhibition determines GA-induced cell growth arrest. Since GA at $<1 \mu\text{M}$ has almost completely inhibited cell viability, we suggest that GA-induced decreased cell viability and cell death rely on proteasome inhibition. However, further studies are needed in order to confirm whether there is any off-target mechanism involved in GA-mediated effect.

GA Is a Cell-Specific Proteasome Inhibitor Compared to Vel

Proteasome inhibition has been used for cancer therapy and Vel has been approved by US Food and Drug Administration for treating multiple myeloma (Richardson et al., 2005; Adams, 2004). As the proteasome exists in all the cells, specific proteasome inhibitors would definitely inhibit the proteasome function to some extent. Therefore, one important approach is to discover new proteasome inhibitors with efficient antitumor effects and cell-specific proteasome inhibition to decrease the toxic side effects. Since the expression of the p450 system in red blood cells and other peripheral blood cells is relatively low or deficient (Choudhary et al., 2005), we hypothesize that GA may not affect the proteasome activity in these cells in vitro and in vivo. GA indeed did not dramatically affect these proteasome activities in low CYP2E1-expressing whole blood cells. However in purified human peripheral mononuclear cells, GA at a higher dose could still induce accumulation of ubiquitinated proteins to some extent, implying the possible existence of P450 enzyme or other enzymes metabolizing GA in human peripheral mononuclear cells. Since proteasome is the specific molecular target of GA, next we compared the effects of GA and Vel on lymphocyte in vitro and in vivo. At their efficient doses, GA did not dramatically affect lymphocyte number both in vitro and in vivo consis-

tent to previous report (Guo et al., 2003), while a high dose of Vel dramatically inhibits lymphocyte number in vitro and in vivo. Consistent to the proteasome inhibition, GA could also induce cytotoxicity to some extent in human peripheral mononuclear cells but much lower than in leukemic cancer cells. Based on these results, we conclude that the specific distribution of CYP2E1 or other related P450 enzyme plays an important role in determining GA-induced proteasome inhibition and cytotoxicity. It was further found that Vel but not GA could induce proteasome inhibition in spleen tissues in vivo. These results confirm that GA induces cell-specific proteasome inhibition compared to Vel.

Cell-specific proteasome inhibition would be significant in designing a novel strategy to overcome multiple proteasome malfunction-related diseases. In clinical cancer chemotherapy including Vel therapy, one of the important side effects is the toxic effect on immune system and hemopoietic system (Richardson et al., 2005; Adams, 2004). First, as expected, CYP2E1 is weakly or even not expressed in mature peripheral lymphocytes and hemopoietic cells (Choudhary et al., 2005). Since these cells lack of CYP2E1 to metabolize GA, it is possible that GA is less toxic on lymphocytes and the hemopoietic system (Guo et al., 2003). Second, all the 60 NCI cancer cell lines displayed high P450 activity including CYP2E1 activity and in six human myeloblastic and lymphoid cell lines (Nagai et al., 2002; Yu et al., 2001), and our results also found that most of the cancer cells have a relatively higher level of CYP2E1 compared with the normal human MSC. Also, the normal tissues express low levels of CYP2E1 except the liver and the kidney (Choudhary et al., 2005), so GA should be an anticancer candidate that is less toxic to normal tissues. Our results further confirm that CYP2E1 is very weakly expressed in bone marrow blood cells from normal humans but highly expressed in bone marrow cells from leukemic patients. Even though therapeutic dose of GA does not dramatically affect the liver and the kidney (Guo et al., 2006), consistent to the CYP2E1 distribution, a toxic dose of GA could affect the function of the liver and the kidney (Qi et al., 2008). Finally, compared with traditional proteasome inhibitors, GA-induced proteasome inhibition is cell- or organ specific, as a specific proteasome inhibitor it will potentially be used in different organ dysfunction. In summary, we have identified GA as a potent proteasome inhibitor and GA-induced cell-specific proteasome inhibition should be of great importance in the future clinical trials.

EXPERIMENTAL PROCEDURES

Peptidase Activity Assay

In vitro CT-like peptidase assay was performed as described with the synthetic fluorogenic peptide Suc-LLVY-AMC purchased from Calbiochem. Cell-based peptidase assay was performed as reported (Huang et al., 2011b). Briefly, cells ($\sim 4,000$ /well) were treated with an indicated agents at 37°C for 6 hr, followed by incubation with the Promega Proteasome-Glo Cell-Based Assay Reagent (Promega Bioscience, Madison, WI) for 15 min. Luminescence was detected with luminescence microplate reader (Varioskan Flash 3001, Thermo, USA).

Models of H22 Allografts and P388 Ascities

All animal protocols used were approved by the Institutional Animal Care and Use Committee of Guangzhou Medical College. The mice were obtained from

Guangdong Laboratory Animal Monitoring Institute (SCXK2008-2002). P388 ascities mouse model was performed as reported (Yang et al., 2009). After 24 hr i.p. inoculation, male KMF mice were treated with i.p. bolus injections of the drug vehicle (10% DMSO, 15% ethanol, and 75% PBS) or GA (1.5 mg/kg) for 7 consecutive days, and kept for additional 60 days to monitor survival daily.

H22 allograft model was performed as described (Yang et al., 2009). Murine H22 cells (10×10^6) suspended in 0.2 ml of RPMI 1640 medium were inoculated s.c. in the left armpit of each mouse. After 24 hr of inoculation, mice (ten mice per group) were treated with either vehicle (10% DMSO, 30% Cremophor, and 60% PBS) or GA (1.5, or 2.0 mg/kg of body weight) via daily i.p. injection for 7 consecutive days, or Vel (1 mg/kg) every 3 days. Two days after the treatment, the mice were sacrificed, and the tumor tissues were weighed.

DNA Microarray Assay and Analysis

HepG2 cells were treated with GA or Vel for 9 hr, and then cells were extracted with TRIzol agents. DNA microarray was performed by Kangchen biotech company (Shanghai) in compliance to MIAME guidelines (for more details, refer to the [Extended Experimental Procedures](#)).

Statistical Methods

Mean \pm SD are presented where applicable. Unpaired Student's t test or one-way ANOVA is used for determining statistic probabilities. p value <0.05 is considered significant.

ACCESSION NUMBERS

The Gene Expression Omnibus accession number for the microarray gene data reported in the paper is GSE38730.

SUPPLEMENTAL INFORMATION

Supplemental Information includes Extended Results, Extended Experimental Procedures, and seven figures and can be found with this article online at <http://dx.doi.org/10.1016/j.celrep.2012.11.023>.

LICENSING INFORMATION

This is an open-access article distributed under the terms of the Creative Commons Attribution-NonCommercial-No Derivative Works License, which permits non-commercial use, distribution, and reproduction in any medium, provided the original author and source are credited.

ACKNOWLEDGMENTS

This work was supported by the National High Technology Research and Development Program of China (Project 2006AA02Z4B5), NSFC (81272451/H1609, 81070033/H0108, 30770835), Key Projects (9251018201002, 10A057S) from Guangdong NSF and Guangzhou Education Commission (to J.L.). J.L. and Q.P.D conceived of the study, analyzed data, and wrote the manuscript; other authors planned experiments or assisted in writing the manuscript or analyzing the data.

Received: March 14, 2012

Revised: June 13, 2012

Accepted: November 27, 2012

Published: December 20, 2012

REFERENCES

Adams, J. (2004). The development of proteasome inhibitors as anticancer drugs. *Cancer Cell* 5, 417–421.

Adams, J., Palombella, V.J., Sausville, E.A., Johnson, J., Destree, A., Lazarus, D.D., Maas, J., Pien, C.S., Prakash, S., and Elliott, P.J. (1999). Proteasome

inhibitors: a novel class of potent and effective antitumor agents. *Cancer Res.* 59, 2615–2622.

Choudhary, D., Jansson, I., Stoilov, I., Sarfarazi, M., and Schenkman, J.B. (2005). Expression patterns of mouse and human CYP orthologs (families 1-4) during development and in different adult tissues. *Arch. Biochem. Biophys.* 436, 50–61.

Feng, F., Liu, W., Wang, Y., Guo, Q., and You, Q. (2007). Structure elucidation of metabolites of gambogic acid in vivo in rat bile by high-performance liquid chromatography-mass spectrometry and high-performance liquid chromatography-nuclear magnetic resonance. *J. Chromatogr. B Analyt. Technol. Biomed. Life Sci.* 860, 218–226.

Groll, M., Bochtler, M., Brandstetter, H., Clausen, T., and Huber, R. (2005). Molecular machines for protein degradation. *ChemBioChem* 6, 222–256.

Gruenewald, T.B.J., and Jaenicke, C. (2000). *PDR for Herbal Medicines, Second Edition* (Montvale, NJ: Medical Economics), pp. 325–326.

Guo, Q.L., Zhao, L., Wu, Z.Q., You, Q.D., Yu, G., and Zhang, Q. (2003). Effect of gambogic acid on the hemopoietic and immune function in experimental animals. *Chin. J. Nat. Med.* 1, 229–231.

Guo, Q., Qi, Q., You, Q., Gu, H., Zhao, L., and Wu, Z. (2006). Toxicological studies of gambogic acid and its potential targets in experimental animals. *Basic Clin. Pharmacol. Toxicol.* 99, 178–184.

Hao, K., Liu, X.Q., Wang, G.J., and Zhao, X.P. (2007). Pharmacokinetics, tissue distribution and excretion of gambogic acid in rats. *Eur. J. Drug Metab. Pharmacokinet.* 32, 63–68.

Huang, H., Chen, D., Li, S., Li, X., Liu, N., Lu, X., Liu, S., Zhao, K., Zhao, C., Guo, H., et al. (2011a). Gambogic acid enhances proteasome inhibitor-induced anti-cancer activity. *Cancer Lett.* 307, 221–228.

Huang, H., Liu, N., Zhao, K., Zhu, C., Lu, X., Li, S., Lian, W., Zhou, P., Dong, X., Zhao, C., et al. (2011b). Sanggenon C decreases tumor cell viability associated with proteasome inhibition. *Front. Biosci.* 3, 1315–1325.

Kot, M., and Daniel, W.A. (2009). Effect of diethylthiocarbamate (DDC) and ticlopidine on CYP1A2 activity and caffeine metabolism: an in vitro comparative study with human cDNA-expressed CYP1A2 and liver microsomes. *Pharmacol. Rep.* 61, 1216–1220.

Liu, Y.T., Hao, K., Liu, X.Q., and Wang, G.J. (2006). Metabolism and metabolic inhibition of gambogic acid in rat liver microsomes. *Acta Pharmacol. Sin.* 27, 1253–1258.

Nagai, F., Hiyoshi, Y., Sugimachi, K., and Tamura, H.O. (2002). Cytochrome P450 (CYP) expression in human myeloblastic and lymphoid cell lines. *Biol. Pharm. Bull.* 25, 383–385.

Pandey, M.K., Sung, B., Ahn, K.S., Kunnumakkara, A.B., Chaturvedi, M.M., and Aggarwal, B.B. (2007). Gambogic acid, a novel ligand for transferrin receptor, potentiates TNF-induced apoptosis through modulation of the nuclear factor-kappaB signaling pathway. *Blood* 110, 3517–3525.

Qi, Q., You, Q., Gu, H., Zhao, L., Liu, W., Lu, N., and Guo, Q. (2008). Studies on the toxicity of gambogic acid in rats. *J. Ethnopharmacol.* 117, 433–438.

Richardson, P.G., Sonneveld, P., Schuster, M.W., Irwin, D., Stadtmauer, E.A., Facon, T., Harousseau, J.L., Ben-Yehuda, D., Lonial, S., Goldschmidt, H., et al.; Assessment of Proteasome Inhibition for Extending Remissions (APEX) Investigators. (2005). Bortezomib or high-dose dexamethasone for relapsed multiple myeloma. *N. Engl. J. Med.* 352, 2487–2498.

Tang, Z.Y., Wu, Y.L., Gao, S.L., and Shen, H.W. (2008). Effects of the proteasome inhibitor bortezomib on gene expression profiles of pancreatic cancer cells. *J. Surg. Res.* 145, 111–123.

Yang, H., Zhou, P., Huang, H., Chen, D., Ma, N., Cui, Q.C., Shen, S., Dong, W., Zhang, X., Lian, W., et al. (2009). Shikonin exerts antitumor activity via proteasome inhibition and cell death induction in vitro and in vivo. *Int. J. Cancer* 124, 2450–2459.

Yang, J., Ding, L., Jin, S., Liu, X., Liu, W., and Wang, Z. (2010). Identification and quantitative determination of a major circulating metabolite of gambogic acid in human. *J. Chromatogr. B Analyt. Technol. Biomed. Life Sci.* 878, 659–666.

- Yang, J., Ding, L., Hu, L., Qian, W., Jin, S., Sun, X., Wang, Z., and Xiao, W. (2011). Metabolism of gambogic acid in rats: a rare intestinal metabolic pathway responsible for its final disposition. *Drug Metab. Dispos.* 39, 617–626.
- Yu, L.J., Matias, J., Scudiero, D.A., Hite, K.M., Monks, A., Sausville, E.A., and Waxman, D.J. (2001). P450 enzyme expression patterns in the NCI human tumor cell line panel. *Drug Metab. Dispos.* 29, 304–312.
- Yi, T., Yi, Z., Cho, S.G., Luo, J., Pandey, M.K., Aggarwal, B.B., and Liu, M. (2008). Gambogic acid inhibits angiogenesis and prostate tumor growth by suppressing vascular endothelial growth factor receptor 2 signaling. *Cancer Res.* 68, 1843–1850.
- Zhang, H.Z., Kasibhatla, S., Wang, Y., Herich, J., Guastella, J., Tseng, B., Drewe, J., and Cai, S.X. (2004). Discovery, characterization and SAR of gambogic acid as a potent apoptosis inducer by a HTS assay. *Bioorg. Med. Chem.* 12, 309–317.
- Zhou, Z.T., and Wan, J.W. (2007). Phase I human tolerability trial of gambogic acid. *Chin. J. New Drugs* 1, 679–682.